Copy No. 7

DEFENCE R&D DÉFENSE

DETECTION PERFORMANCE OF THE STEERED, ADAPTIVE, SUBARRAY BEAMFORMER

D.N. Swingler

SAINT MARY'S UNIVERSITY

DEFENCE RESEARCH ESTABLISHMENT ATLANTIC

Contractor Report

DREA CR 1999-004

January 1999

Défense nationale National Defence

Canada

National Defence
Research and Development Branch

Défense nationale
Bureau de recherche et développement

DREA CR 1999/004

DETECTION PERFORMANCE OF THE STEERED, ADAPTIVE, SUBARRAY BEAMFORMER

D.N.Swingler

SAINT MARY'S UNIVERSITY
Engineering Division
Halifax, Nova Scotia, Canada
B3H 3C3
Address

Scientific Authority
I.A.Fraser

W7707-7-5425
Contract Number

January 1999

CONTRACTOR REPORT

Prepared for

Defence Research Establishment Atlantic

Centre de Recherches pour la Défense Atlantique

Canada

ABSTRACT

The detection performance of the steered, minimum variance, subarray beamformer is examined via numerical simulations, with specific reference to the impact of four different subarray geometries. Additionally the advantages of employing a quadratic constraint are examined. The measures used to elucidate performance include output SNR, array gain, and the detection index. The most salient result is that the beamformer with contiguous subarrays of differing lengths (referred to herein as SA2M), and its quadratically-constrained counterpart, appear to offer the best overall performance in terms of their ability to null close interferers while offering freedom from the type of artifacts that potentially bedevil the other subarray beamformers under test.

RÉSUMÉ

Le rendement de détection du formeur de faisceau dirigé à module à variance minimale est examiné par de nombreuses simulations numériques en faisant référence à l'impact de quatre géométries de module différentes. De plus, les avantages de l'utilisation d'une contrainte quadratique sont examinées. Les mesures utilisées pour élucider le rendement comprennent le SNR de sortie, le gain du faisceau et l'indice de détection. Le résultat le plus significatif est que le formeur de faisceau avec des modules continus de différentes longueurs (désigné SA2M dans l'étude) et sa contrepartie à contrainte quadratique semblent offrir le meilleur rendement global en termes de capacité en présence de brouilleurs tout en ne dépendant pas du type d'artéfacts qui gênent les autres formeurs de faisceaux des sous-modules à l'essai.

Detection Performance of the Steered, Adaptive, Subarray Beamformer

Executive Summary

- A basic action of multisensor sonars is to reject unwanted signals and noise and to determine the arrival angles of desired signals. These objectives are normally met simultaneously by pre-forming narrow beams that cover all potential signal arrival directions. A potential deficiency of this technique is that interfering noise is often not sufficiently well rejected by the spatial filtering provided by "conventional" fixed-response beamformers. Over the years a great deal of effort has been devoted to devising "adaptive" beamformers that adjust the spatial filter characteristics in response to the incoming signals to optimize the beamformer's performance in a desired manner. This effort has met with rather meagre success, partly because of the large additional computational load imposed by the adaptive process, but more importantly because the "real" ocean presents an acoustic environment that is more complex than fully adaptive beamformers can deal with. Another constraint on adaptive beamformer design is the need for nearly instantaneous adaptation to the very dynamic reverberation and noise fields associated with low-frequency active sonar and active jammers, respectively. A very few partially adaptive, more robust beamforming techniques have been devised in recent years to overcome many of the above-mentioned problems. One of the most promising of these techniques is the steered, minimum-variance subarray (STMV-SA) beamformer. Its performance in various guises in a variety of simulated ocean environments is the subject of this paper.

- The STMV-SA beamformer is a partially adaptive beamformer whose number of adaptive degrees of freedom may be much less than the number of sensors in the array. Given that the performance of such a beamformer improves as the ratio of the number of adaptive degrees of freedom to the time-bandwidth product of the processed data decreases, such a beamformer is of interest in situations where the observation time is short.

- The three key facets of the STMV-SA beamformer are: (1) a reduction in the number of adaptive degrees of freedom by utilizing in the adaptive process only the outputs of a relative small number of "delay-and-sum" beamformers, each formed on taking a different subset of the sensors of the original array, here

assumed to be a uniform line-array; (2) the concomitant reduction in dimensionality and computational loading of the adaptive processing; and (3) the utilization of wideband input data through the use of the steered-covariance matrix formulation, which in essence implies a simple pre-steering of the array to the bearing of interest.

- In a previous report [Swingler, D.N., DREA Contractor Report CR/98/draft] it was found that the performance of the STMV-SA beamformer was sensitive to the choice of subarray structure. Four choices are examined here, incuding one with overlapped, equi-length subarrays, as proposed by Dhanatawari and Stergiopoulos [DREA Contractor Report CR/96/450]; the best performance was obtained by modifying a sub-array structure proposed by Owsley [Owsley, N.L., "Systolic array beamforming," NUSC Report 7891]. Instead of dividing the array into a set of equal length contiguous subarrays, as Owsley proposed, the contiguous subarrays are made unequal in length, thereby largely eliminating a grating-lobe type of interference, while at the same time offering reasonable suppression of close interferers. This technique also appears to be more tolerant of defective sensors than other sub-array schemes.

- If a finite amount of data is available for determining the adaptive weights, the adaptive beamformer performance can be degraded by what is known as the "misadjustment effect." A standard technique for reducing this unwanted effect is by imposing a quadratic constraint on the sample covariance matrix that is used in the adaptive-weight calaculation. Again the modified Owsley sub-array structure appears to provide better interference rejection near the look direction than do the other sub-array techniques.

- Although the STMV-SA beamformers all tend to operate better than most other adaptive beamformers, especially in dynamic noise and reverberation environments, they still suffer, as members of the MVDR (minimum variance directional response) class of beamformers, from the multipath signal-cancellation problem when two or more signals of the same frequency are received. Hence it still appears to be unwise to place total dependence upon adaptive beamforming for spatial filtering in a sonar. Rather it should be made available for use in cases where interference is strong and nearly discrete in arrival direction.

LIST OF CONTENTS

1. Introduction 1-1

2. Subarray structures revisited 2-1

2.1 Introduction 2-1
2.2 Some infinite-time results 2-2
2.3 Experiment with a missing sensor 2-5
2.4 Overall summary 2-5
2.5 Appendix: Details of the SA2M processor 2-6

3. Some misadjustment experiments 3-1

3.1 Introduction 3-1
3.2 Misadjustment experiments 3-1
3.3 Experiments with a quadratic constraint 3-4
3.4 Summary 3-5

4. Detection index experiments 4-1

4.1 Introduction 4-1
4.2 Detection index experiments 4-1
4.3 Summary 4-5

5. Conclusion 5-1

6. References 6-1

1. Introduction

This brief report is concerned with the detection performance of the so-called steered, minimum-variance, subarray beamformer (STMV-SA) line-array beamformer which was itself the subject of two earlier DREA Contractor's Reports [1-1, 1-2]. In particular, we examine several variants of the original STMV-SA beamformer [1-2] where the variations relate to differing subarray geometries.

The original subarray geometry of Owsley [1-3] used non-overlapped but contiguous, equal-length subarrays to form what is referred to as the SA2 beamformer. This was later modified by Dhanatawari [1-2] who used heavily overlapped equal-length subarrays to form the SA1 beamformer. In [1-1] we introduced a third structure, SX, (in this report referred to as SAX) where the subarrays are formed by selecting elements *at random* from the underlying line-array. In this report we also introduce a modified Owsley structure (SA2M) to alleviate some of the performance problems observed in the SA1, SA2 and SAX beamformers, as detailed in [1-1]. For the underlying mathematical details of the various SA beamformers, the reader is referred to [1-1].

The structure of the report is as follows: In Section 2 we examine the infinite-time performance of the beamformers in terms of familiar measures such as array-gain improvement (AGI) and output SNR. In Section 3 we move into the area of finite-time performance where we deal with the misadjustment phenomenon which, *inter alia*, places a ceiling on the maximum output SNR. The advantages of a quadratically-constrained version of the SA beamformer are also explored. In Section 4 we examine finite-time detection performance using the detection index measure. The report terminates in Section 5 with some concluding remarks.

We shall demonstrate that the SA2M beamformer seems to offer the best overall performance.

2. Subarray Structures Revisited

2.1 Introduction

We are concerned here with re-investigating the issue of an "optimum" structure for the subarrays in the Steered Adaptive Subarray Beamformer [1-1]. In particular, we seek a structure that is (a) simple and (b) offers good overall performance. By "simple" we mean that an element from the original line array should either be selected or not for use in a particular subarray. Its gain is assumed to be unity. This eliminates from contention the infinite number of subarrays whose individual elements are allowed to have arbitrary weights. The issue of missing or faulty sensors will be addressed later. The overall array is pre-steered to the direction of interest and for each subarray the unity-gain sensor outputs are simply summed. MVDR-type beamforming is then performed on these subarray outputs to produce a low-complexity adaptive beamformer. In this report we shall also be interested in beamforming in the presence of "close" interferences, where "close" is roughly defined as one-half of a conventional beamwidth from the desired signal.

We shall focus on four basic structures:

(i) Dhanatawari/Stergiopoulos structure [1-2] where each subarray contains exactly N_s consecutive elements from the original array. Each subarray heavily overlaps its neighbour with N_s-1 elements in common. This will be called the SA1 structure.

(ii) The original Owsley structure [1-3] where each subarray contains an equal number of elements but the subarrays are not overlapped. They do however form a contiguous set. This will be known as the SA2 structure.

(iii) A modified Owsley structure where the subarrays form a contiguous (non-overlapped) set but now the number of elements per subarray is not the same for each subarray[1]. This is the SA2M structure.

(iv) A randomised structure where each subarray's elements are chosen randomly from the original array. Each original element is used once and only once and hence will appear in only one subarray. This structure was the result of previous experimentation in connection with the foregoing contract. [1-1]. This is the SAX structure.

We shall describe the results of some "infinite time" calculations where the field covariance matrix is assumed to be known, and will demonstrate that the SA2M approach seems to be the most promising of the four candidates.

2.2 Some Infinite-Time Results

In this Section we are essentially repeating the experiments of Chapter 2 of [1-1]. However, greater attention will be paid to performance differences, particularly for close interferers. It should also be mentioned that the SA2M and SAX methods were not covered explicitly in the previous infinite-time studies. In the interest of brevity, we shall not repeat the mathematical details of the STMV-SA beamformer. They can, of course, be found in [1-1].

We begin by re-establishing the scenario examined in Chapter 2 of [1-1]. There is a plane-wave, narrowband (NB) signal in the pre-steered look-direction with SNR = 10dB. A plane-wave NB interferer is present and its location and interference-to-noise ratio (INR) are varied. The temporal frequency of the interferer is *not* that of the source. The varying location of the interferer translates to a varying spatial frequency, υ_i. The background noise is uncorrelated.

[1] See Appendix 2.5 for more details of the SA2M structure.

First we examine the output from the selected subarray beamformer at the signal frequency and compare it to the performance of a classic, fully-adaptive, NB-MVDR (also known as NBMV) beamformer operating at the same frequency. In Fig. 2.1 we show array-gain improvement (AGI) curves for the STMV-SA1 (hereafter simply referred to as SA1) beamformer and for the NBMV beamformer. The array-gain comparison is made against a Hamming beamformer (CB) operating at the signal frequency. There are three curves for each beamformer, corresponding to INR = {0, 10, 20}dB. As in [1-1] we choose N =24 sensors, N_s = 4 subarrays, M=24 FFT bins.

In Fig. 2.1 we observe that the NBMV curves collapse to a single horizontal line with AGI(NBMV,CB) = 1.3dB, as expected. At large values of spatial frequency, υ_i, the SA1 adaptive beamformer (ABF) is about 0.3dB worse that the NBMV. This small loss is inherent in the subarray method. At smaller values of spatial frequency we note a significant deterioration in performance which is exacerbated as the INR increases. If we define "close" interference to be that for which the spatial frequency $\upsilon_i = 0.5*2\pi/N \approx 0.13$ then we see from Fig. 2.1 that there is a AGI loss of about 5dB at this point for the SA1 beamformer with INR = 20dB. This is due entirely to the SA1 adaptive weights having to increase to deal with the close and strong interferer, even though it is at a different *temporal* frequency. The CB and NBMV beamformers are truly narrowband and do not "see" the interference at all.

In Fig. 2.2 we consider the SA2 ABF and we note that at larger values of spatial frequency, the SA2 ABF is not quite as good as the SA1, particularly near $\upsilon_i = 2\pi/6 = \pi/3$. This was discussed in [1-1]. However, we see that the problems for the close interference are actually slightly reduced; the dips near the left-hand side of the figure are somewhat narrower than those for the SA1 ABF in Fig. 2.1.

In Fig. 2.3 we have the results for the modified SA2M ABF. Here the four subarray lengths are not {6, 6, 6, 6} as for the SA2 ABF, but are actually {4, 5, 6, 9}.

This choice destroys the regular SA structure that causes the SA2 problems near its grating lobes [1-1]. For this reason the SA2M performance for larger values of spatial frequencies on Fig 2.3 is a little better than the SA2 of Fig. 2.2 while the performances at small values of spatial frequency are comparable.

For completeness we present the results in Fig. 2.4 for the STMV-SAX beamformer where the subarray elements are chosen randomly. Again we note the trade-off of good performance at larger values of spatial frequency for inferior performance at low spatial frequencies.

We now move on to examine beamformer performance at the interference frequency. Unlike the previous case, all the beamformers are now exposed to the interferer. We start with Fig. 2.5 which represents the interference-to-noise improvement (IGI) for the SA1 vs. the CB. Again we observe that the SA1 performs about as well as the fully-adaptive NBMV benchmark for larger spatial frequencies. However for lower spatial frequencies the SA1 is generally inferior. Note that both adaptive beamformers have significant gain over the CB at spatial frequencies inside those corresponding to the edge of the Hamming BF's mainlobe, i.e. within $2*2\pi/N = \pi/6 \approx 0.5$. The SA1 however has a "glitch" near $\upsilon_i = \pi/21 \approx 0.15$, a null point for the sidelobe structure of each of the 21-element subarrays, and inside this value its performance is significantly worse than the NBMV. Interestingly, this is particularly noticeable for the weaker INR's.

In Fig. 2.6 we have the corresponding results for the SA2 BF. We see significant problems for larger spatial frequencies (the grating lobe effect [1-1]) but we also note that the performance for low spatial frequencies is better than the SA1 in Fig. 2.5.

Moving to the SA2M, we have the results in Fig. 2.7. Here we see that the impact of having different lengths of non-overlapping subarrays is to reduce the grating lobe problems of the SA2 observed in Fig 2.6 while simultaneously improving the results for low values of spatial frequencies relative to the SA1 BF in Fig. 2.5. It would seem then

that the SA2M beamformer is a good compromise when taken over both large and small spatial frequencies.

Finally we present the SAX results in Fig. 2.8. The major problem with the SAX results lies in the inferior performance for low spatial frequencies.

2.3 Experiment with a missing sensor

In [1-1] it was demonstrated that the SA1 ABF was susceptible to significant problems related to missing sensors. For example, Fig. 2.9 shows the SA1 AGI curve where the parameters are as above but with N_s increased (arbitrarily) to N_s=7 (i.e. six degrees of freedom) and sensor #7 is missing. We immediately note the resulting deep nulls at $p2\pi/N_s = p2\pi/18 \approx 0.35\pi$ where p is integer as discussed in [1-1]. We also note the relatively poor performance for low values of spatial frequency. The considerable elevation in overall IGI level for spatial frequencies greater than $\upsilon_i \approx 0.5$ and for INR = 20dB is due to the ability of each ABF to reject the interference (except at the null locations) while the missing sensor causes an increase in the corresponding sidelobe levels of the CB.

In Fig. 2.10 we have the corresponding result for the SA2M beamformer where we note that the deep nulls are absent and that the performance for low values of spatial frequency has improved.

Finally, in Fig. 2.11 we have the SAX result. Again the performance for large values of spatial frequency is good, but the performance for smaller values is weak.

2.4 Overall Summary

These experiment suggest that the best overall choice of beamformer is the SA2M beamformer. It does not suffer strong grating-lobe-type problems for larger values of

interference spatial frequency, yet offers reasonable suppression for close interference. It also seems tolerant of missing sensors.

2.5 Appendix: Details of the SA2M structure

In the basic Owsley (SA2) method, we have $N_s = N/N_a$ sensors per subarray. However, this regular arrangement gives rise to grating-lobe problems and the rationale behind the SA2M method is to simply "jitter" the subarray lengths so that they are not all the same. After some trial-and-error, it was observed that a reasonable approach is to select the subarray lengths such that they range between 70% and 130% of N/N_a. Hence, on average, the subarray length is that of the SA2 beamformer. It is not always possible to exactly satisfy the jitter condition. For instance, for $N = 24$, $N_a = 4$, we have the subarray lengths as {4, 5, 6, 9}.

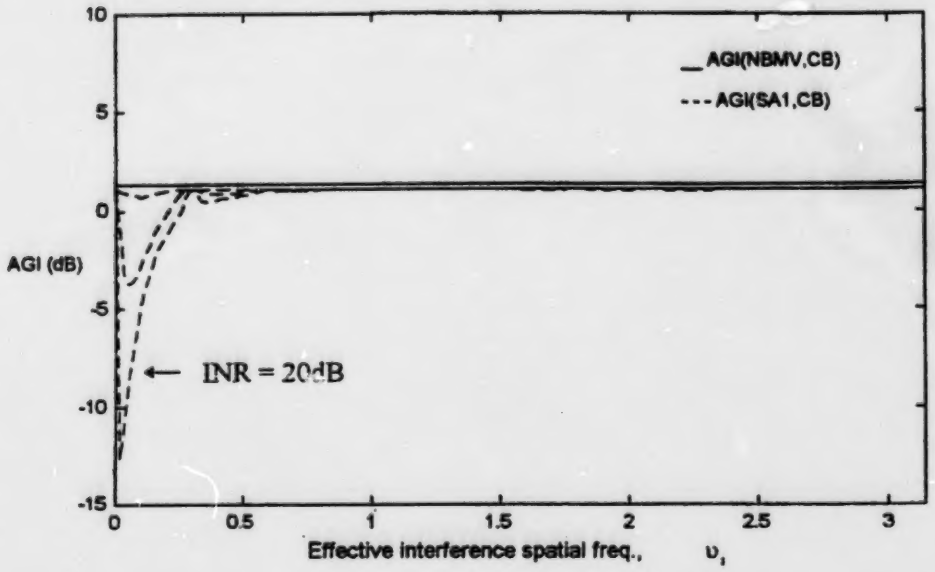

Fig. 2.1 SA1 AGI curves at signal frequency. N=24, N_a=4, INR={0, 10, 20} dB

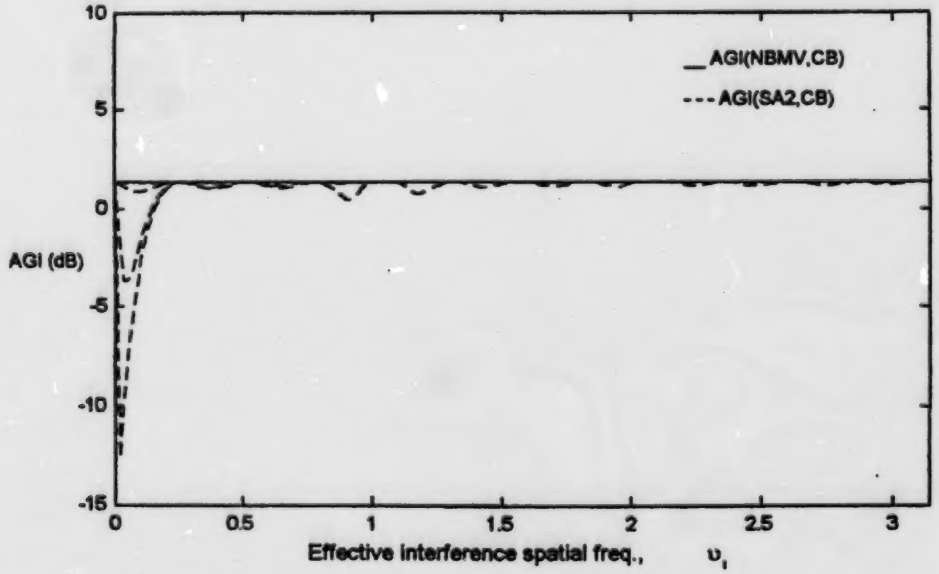

Fig. 2.2 As Fig. 2.1 but using the SA2 processor of Owsley.

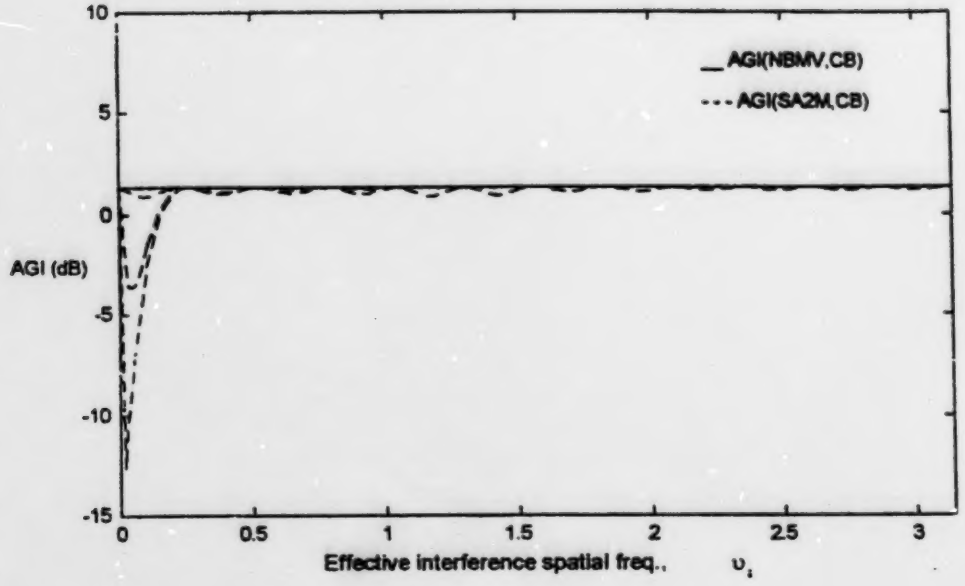

Fig. 2.3 As Fig. 2.1 but using the SA2M processor.

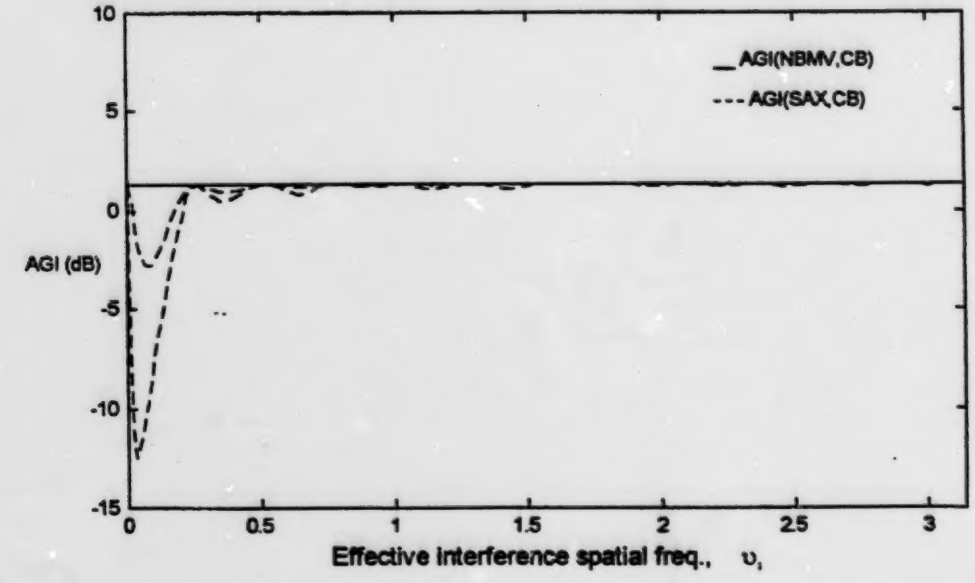

Fig. 2.4 As Fig. 2.1 but using the SAX processor with randomised subarray elements.

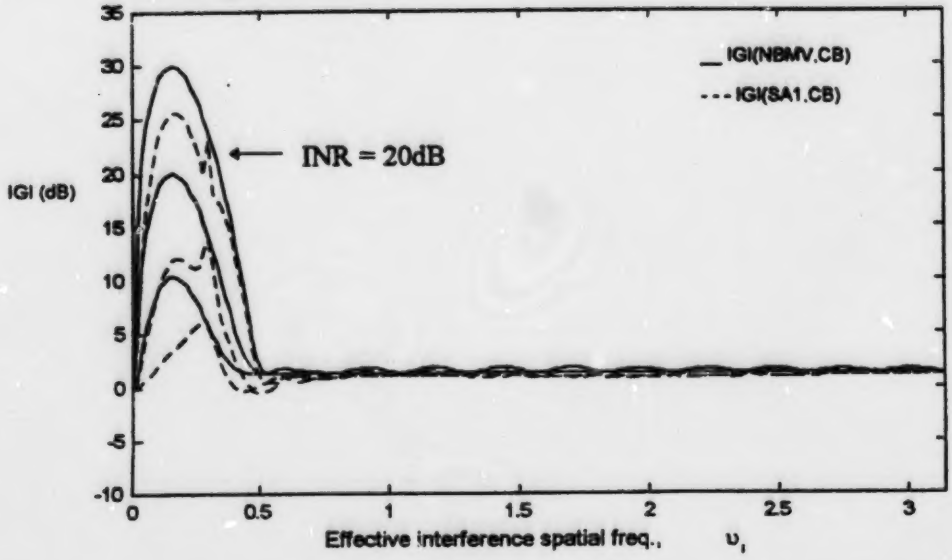

Fig. 2.5. SA1 IGI curves at the interference frequency. Note inferior performance of SA1 processor for low values of spatial frequency. N=24, N_s=4, INR={0, 10, 20} dB

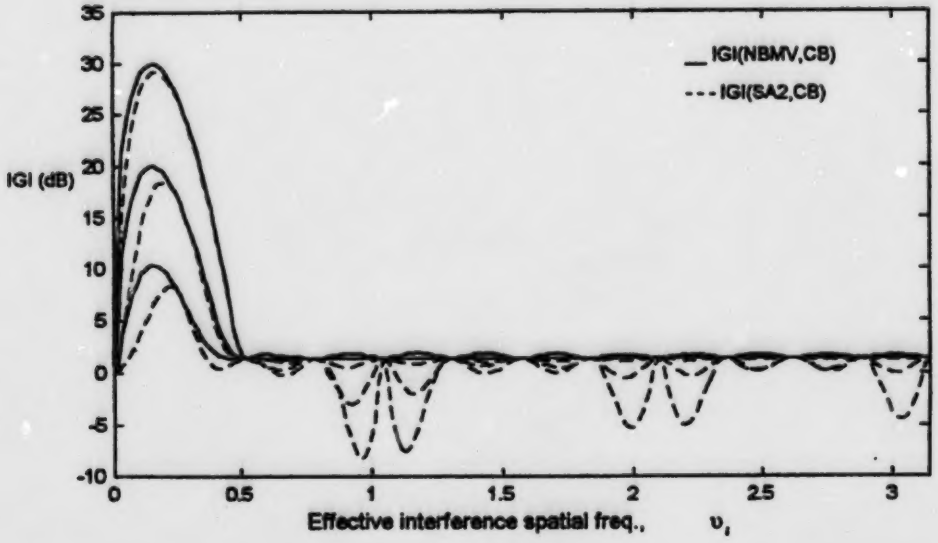

Fig. 2.6 As Fig. 2.5 but with the SA2 processor. Note the significant problems near the grating-lobe locations but improved performance for low spatial frequencies.

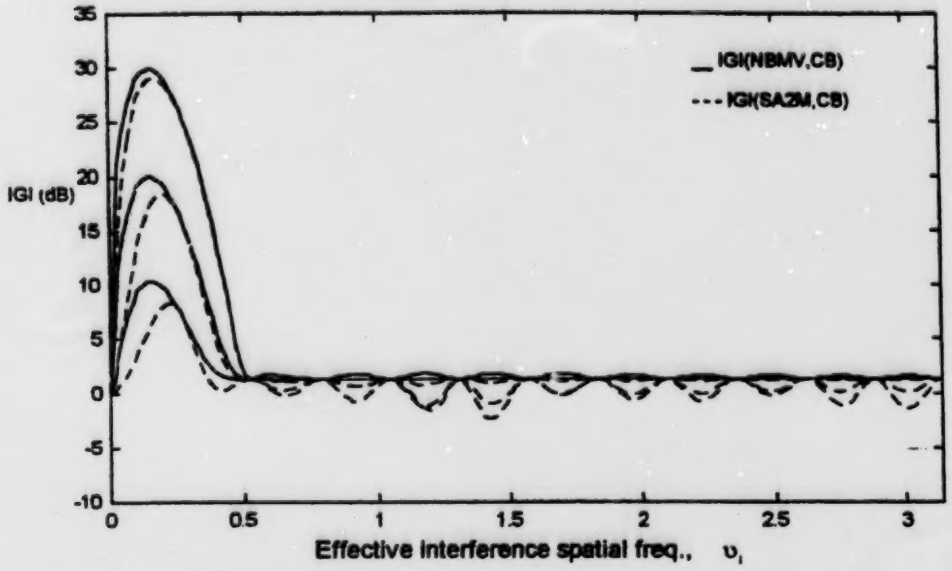

Fig. 2.7 As Fig. 2.5 but using SA2M processor. The grating lobe problems are ameliorated and the performance at low spatial frequencies is acceptable.

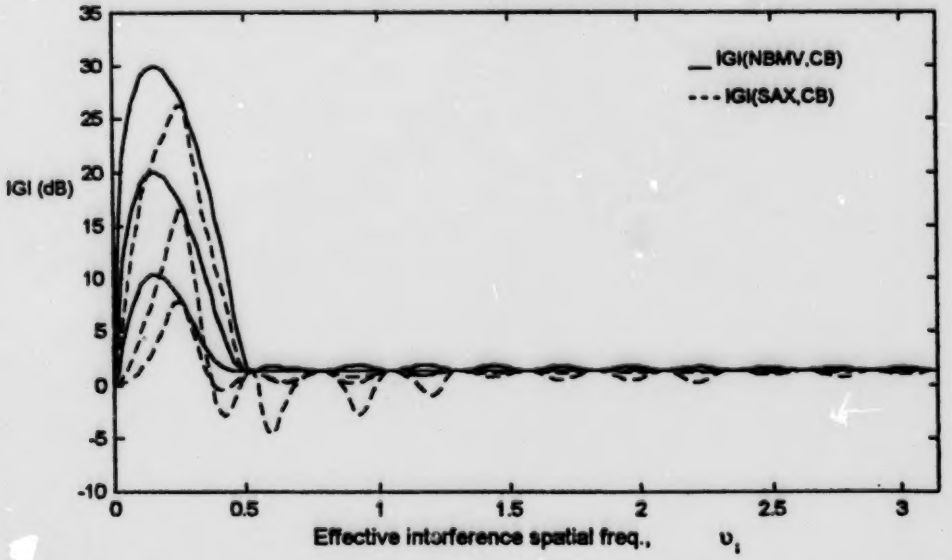

Fig. 2.8 As Fig. 2.5 but with the randomised SAX processor. Again note the inferior performance for low spatial frequencies.

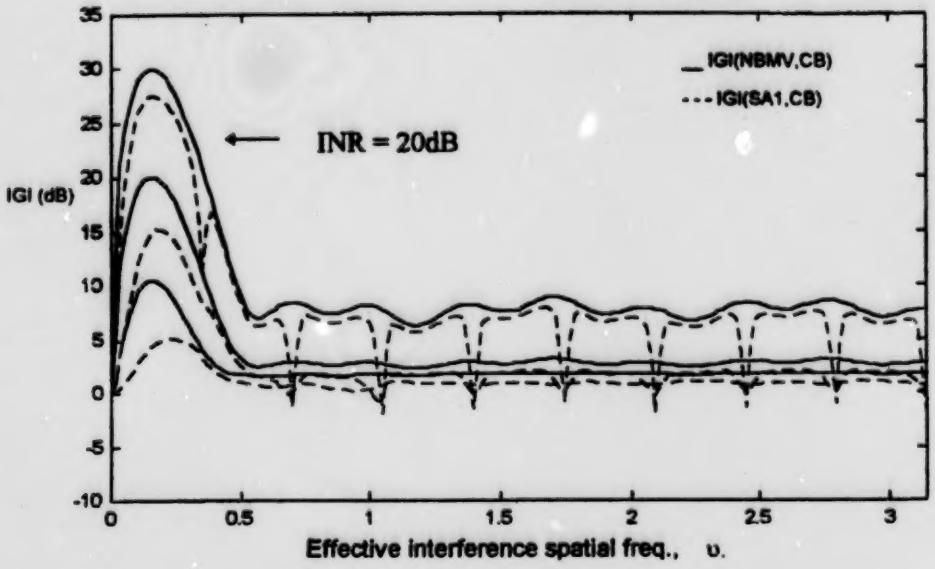

Fig. 2.9 IGI curves for SA1 BF with N_s=7 and sensor #7 missing. Note the regular set of deep nulls.

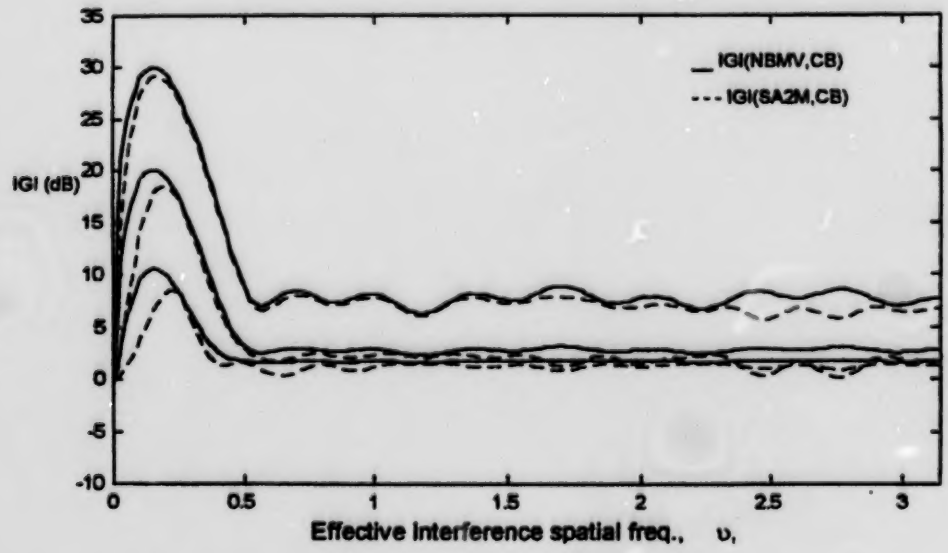

Fig. 2.10 As Fig. 2.9 but for SA2M. Note improvement over Fig. 2.9.

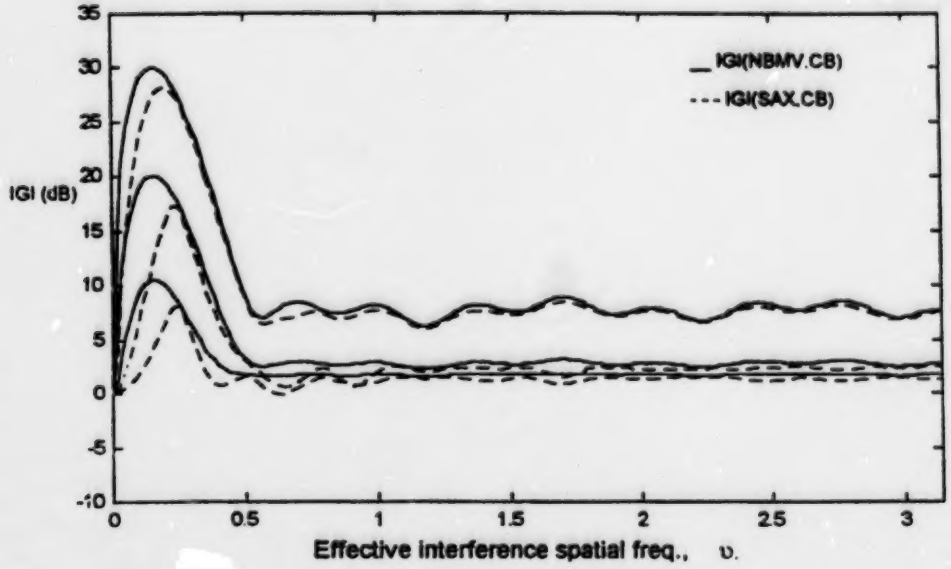

Fig. 2.11 As Fig. 2.9 but for the SAX beamformer. Again note the inferior performance for low values of υ_i.

3. Some Misadjustment Experiments

3.1 Introduction

In the previous section, we presented some NB "infinite-time" results indicating that the SA2M (modified-Owsley) SA beamformer was best performer overall. We now turn our attention to the "finite-time" case where we must estimate the "steered covariance matrix" (STCM) from a finite amount of data. This leads to the so-called "misadjustment" effect where the adaptive weights become a strong function of the SNR of the desired signal. It will be of interest here to compare the performance of the Dhanatawari/Stergiopoulos SA1 beamformer against that of the SA2M. We shall look at the impact of the SNR of the strong signal and also at the impact of a strong, close NB interferer. Finally, we investigate the effect of limiting the weight norm by using a quadrature constraint which, in practice, means adding a constant along the main diagonal of the STCM [3-1].

3.2 Misadjustment Experiments

We modify the experiments of the previous section by *estimating* the STCM matrix from M=24 NB Fourier vectors. In practice, this is equivalent to using the data from 24 adjacent FFT bins. One of these bins contains signal information, another contains interference contributions; this is equivalent to the signal and interference occupying different temporal frequencies. All of the bins contain uncorrelated background noise. This approach was fully discussed in a previous contractor's report [1-1].

The underlying array has N = 24 sensors and we use N_a = 4 subarrays. The interference INR is 20dB and the spatial frequency of the interference is π/N, i.e. it is at one-half of a beamwidth of an unshaded CB from the desired signal, or at about one-

quarter of a beamwidth of a Hamming-shaded CB. The SNR of the signal is varied from -10dB to 20dB in 5dB steps.

We shall look at the response at each of our two beamformers at each of three frequencies (i.e at each of three FFT bins) - one at the signal frequency, one at the interference frequency, the third at a noise-only frequency.

We start with the SA1 beamformer output at the signal frequency. The output SNR is shown in Fig. 3.1 plotted against the input SNR. The results are averaged over 400 realisations. The measured SA1 beamformer output is shown as the solid curve which tends to lie below the points indicated by stars which represent the theoretical output SNR's for the SA1 beamformer in the absence of the interferer, as described in [1-1]. When the input SNR is low, at -10dB, the output SNR lies about 4-5dB below the level which might be expected if there were no interference. This is a consequence of the SA1's weight norm increasing to null the interference. As the input SNR increases, the SA1's output SNR flattens out due to the increase in weight norm related to signal strength effects [1-1]. This is the misadjustment phenomenon.

On Fig. 3.1 we also show the corresponding results (dot-dashed line [experiment] and "+" [theory] symbols) from a fully-adaptive NBMV beamformer where all M=24 vectors have both noise and signal components (but not interference, as it is at a different temporal frequency). These curves flatten out at a much lower level that the SA1 method [1-1]. We also show the output from a Hamming-shaded CB (dashed line [experiment] and "o" [theory] symbols) operating at the signal frequency. This has the best performance as there can be no misadjustment effect for a CB.

In Fig. 3.2 we show the corresponding families of curves for the output from one of the noise-only frequencies. For convenience, these results are normalised by the expected noise power output from the Hamming-CB. At low input SNR, the NBMV's normalised output level is about -1.3dB as expected. The output from the SA1 is

considerably higher as the weight norm has, as mentioned above, increased as it, unlike the NBMV, is forced to deal with strong, close interference. The "*" symbols again relate to the theoretical, finite-time, output level in the absence of the interferer. As the input SNR becomes large, the weight norms of both adaptive beamformers increase and the noise output levels increase. This is the unwelcome misadjustment effect. The CB curves lie at about the 0dB level, as expected.

Fig. 3.3 contains results relating to the output at the noise plus interference frequency. Again the results are normalised by the expected output noise level of the Hamming-CB. The goal here for the SA1 is that these values should be about 0dB, indicating that there is perfect interference suppression with no adverse side effects. We immediately note that the CB output is at about 31dB as the interference is well within its mainbeam. The SA1 beamformer has an output level of about 1dB for low SNR, indicating good interference suppression until the input SNR is in excess of about 10dB where the misadjustment effect plays a role.

We now repeat these experiment using the SA2M beamformer in place of the SA1. In Fig. 3.4 we note that, at low input SNR, the output of SNR of the SA2M beamformer is about 2.5dB lower than the CB, or about 2dB better than the SA1. This might be anticipated from the infinite-time results of the previous section and indicates that the weight norm of the SA2M does not have to increase as dramatically as the SA1 to deal with the close interference. For higher input SNR levels, the output curve for the SA2M beamformer again flattens out. These results are confirmed by those of Fig. 3.5 where we note for low input SNR that the output noise power level is lower than for the SA1 result in Fig. 3.2.

Fig. 3.6 is especially interesting as it clearly demonstrates the ABF's finite-time, noise-quieting effect for low input SNR and high INR. Recall that we might reasonably expect the output SNR to be at about 0dB. However, Fig. 3.6 clearly shows (for low

SNR_{in}) an SA2M output level in the interference plus noise bin of about -7dB. This effect was also observed in [1-1].

Summary: We have demonstrated that the SA2M beamformer is superior to the SA1 ABF in finite-time performance with a strong, close interferer.

3.3 Experiments with a quadratic constraint

In another contractor's report [3-1], it was demonstrated that the introduction of a quadratic constraint is effective in limiting the weight norm for an adaptive beamformer. In practice, this simply means adding an appropriate constant along the main diagonal of the covariance matrix prior to inversion. The following experiments are intended to demonstrate that this is a useful technique for use with our subarray beamformer(s).

In Fig. 3.7 we repeat the SA1 experiment of Fig. 3.1 but utilise a quadratic constraint (QC) such that the weight norm is always less than twice the weight norm in a noise-only scenario. In the noise-only case, each sensor weight is close to 1/N. In Fig. 3.7, at low input SNR, we note that the solid curve (SA1-QC) is now within about 1dB of the CB line, indicating a decreased weight norm relative to Fig. 3.1. We also note that the solid line does *not* plateau for higher input SNR's, another benefit of constraining the weight norm. This is consistent with the solid line on the noise power output graph, Fig. 3.8, being at about the +1dB level across the entire figure. The "*" symbols from the previous figures are retained on Fig. 3.8 for convenience. No constraint is applied to the NBMV results.

The price paid for the quadratic-constraint benefits is visible in Fig. 3.9 where we note that the SA1-QC's output power level at the interference frequency is now about 22.6dB, indicating that the SA1-QC's ability to null out the interferer has been severely compromised by the introduction of the weight constraint.

We now examine the use of the quadrature constraint in conjunction with the SA2M beamformer. The hope is that, because the SA2M does not have a weight norm increase as large as those of the SA1 to deal with the interferer, then its action is less likely to be compromised by the use of the quadratic constraint.

In Fig. 3.10 we have the output SNR for the SA2M-QC beamformer (solid line) in the signal bin. Again we note that it is quite close to the CB, suggesting only a modest loss in SNR due to the effect of the interferer (at low input SNR's) or to the increase in weight norm (at large input SNR's). This is consistent with the noise power output of Fig. 3.11 where again we have output levels for the SA2M-QC of a modest 1dB across all input SNR's.

Finally, we have the interference bin output powers of Fig. 3.12. Unlike the SA1-QC results of Fig. 3.9 where we had SA1-QC output powers in the order of 22dB, we now have for low input SNR's the noise-quieting level of about -6dB showing that there is suppression of the close and strong interferer. For higher input SNR's the SA2M-QC output level does increase, but remains well below the levels observed in the SA1-QC case.

3.4 Summary

It has been demonstrated that the use of a quadrature-constraint in connection with the SA2M beamformer provides a significant degree of misadjustment control without unduly compromising its ability to null out a close, strong plane-wave interferer.

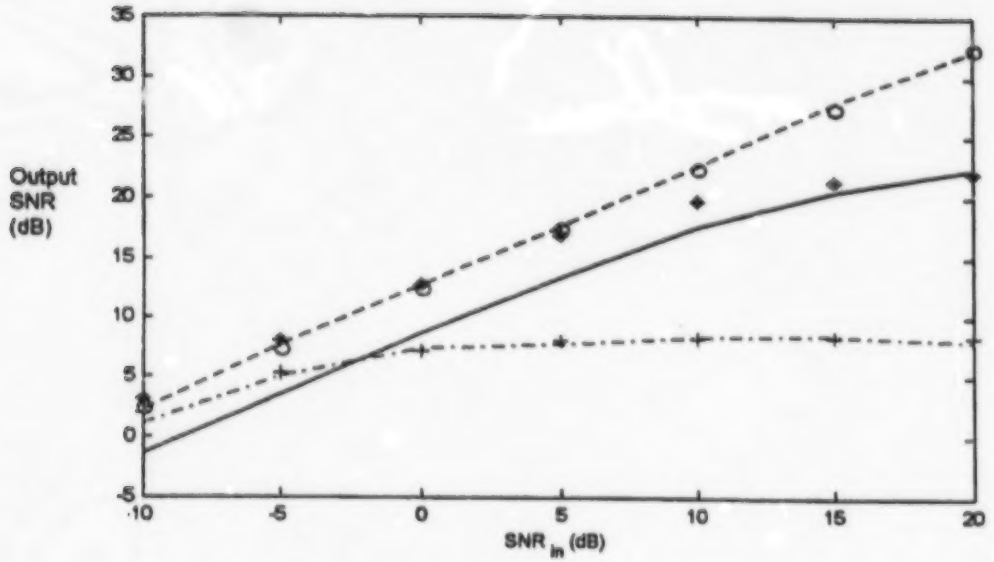

Fig. 3.1 Output SNR at signal frequency. N=24, M=24, INR=20dB, $\upsilon_t = \pi/N$, N_s=4.
(- - and o) = Hamming CB, (__ and *) = SA1, (-.-. and +) = NBMV.

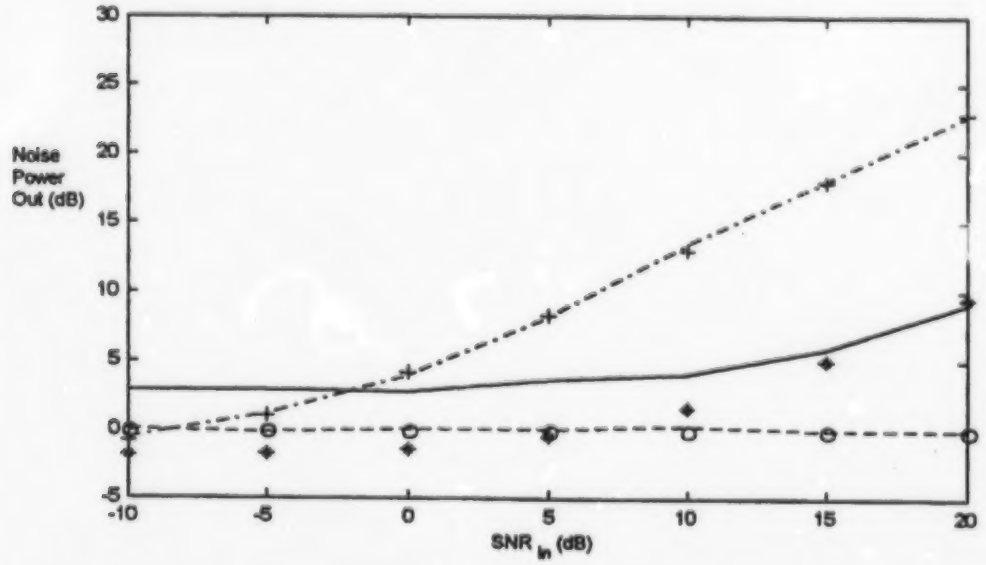

Fig. 3.2 Output power at noise-only frequency for SA1 beamformer.
(- - and o) = Hamming CB, (__ and *) = SA1, (-.-. and +) = NBMV.

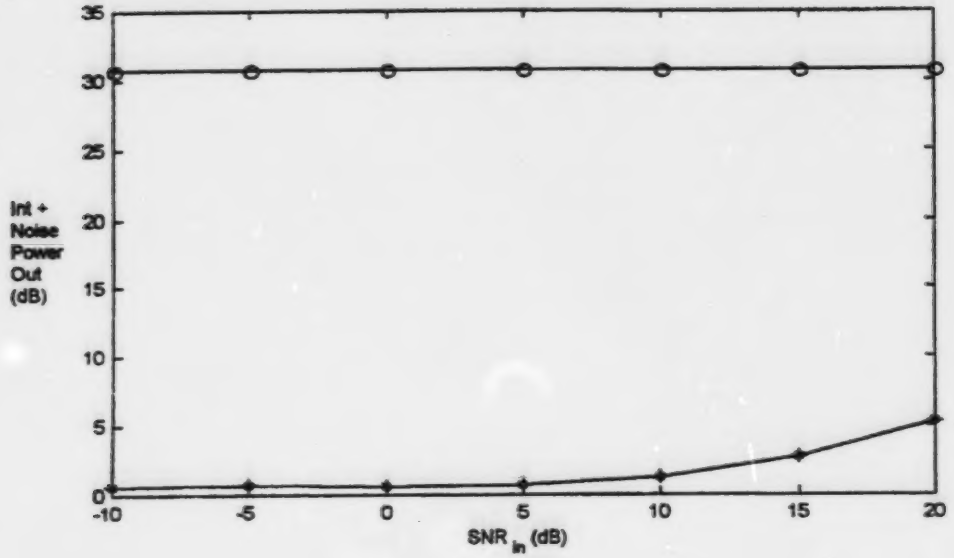

Fig 3.3 Output power at interference plus noise frequency for SA1 beamformer.
ooo = Hamming-CB, *** = SA1 beamformer

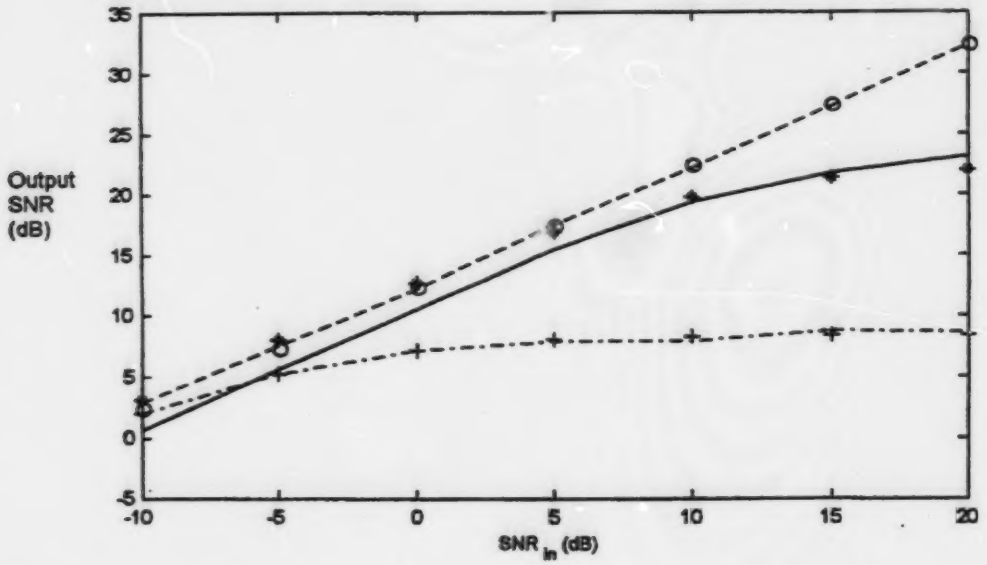

Fig 3.4 As Fig. 3.1 but for SA2M beamformer
(- - and o) = Hamming CB, (__ and *) = SA2M, (-.-. and +) = NBMV.

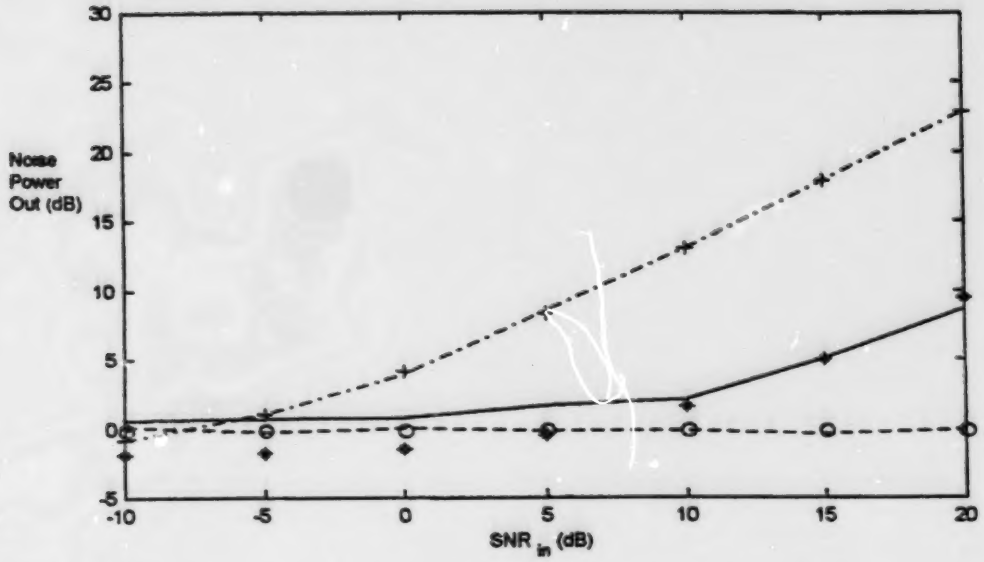

Fig. 3.5 Output power at noise-only frequency for SA2M beamformer.
(- - and o) = Hamming CB, (__ and *) = SA2M, (-.-. and +) = NBMV.

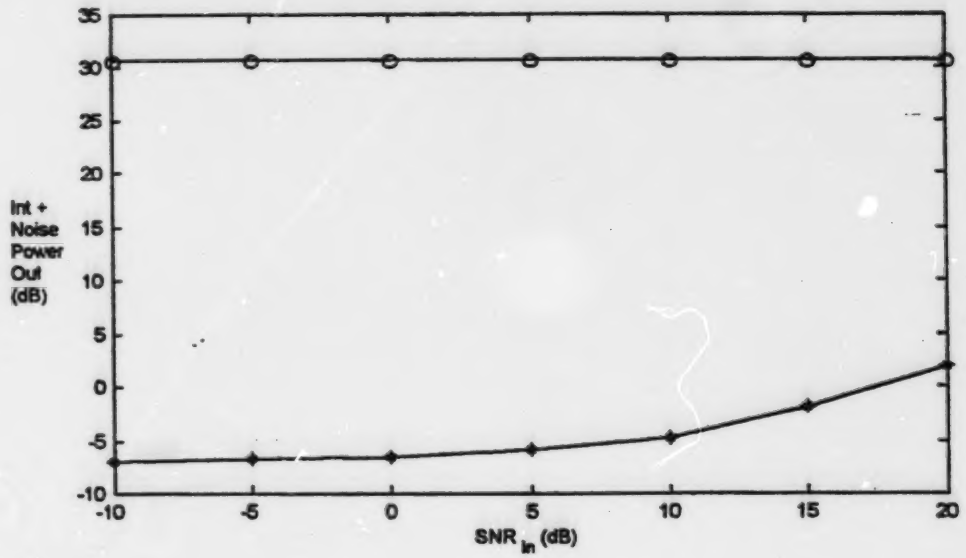

Fig 3.6 Output at interference plus noise frequency for SA2M beamformer.
ooo = Hamming-CB, *** = SA2M beamformer.

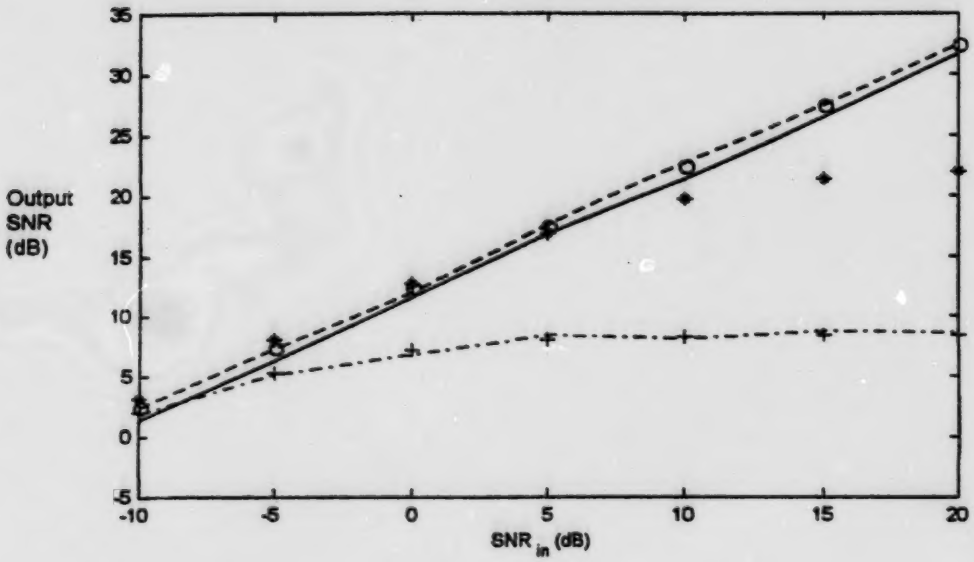

Fig 3.7 Output SNR from SA1-QC beamformer
(- - and o) = Hamming CB, (__ and *) = SA1-QC, (-.-. and +) = NBMV.

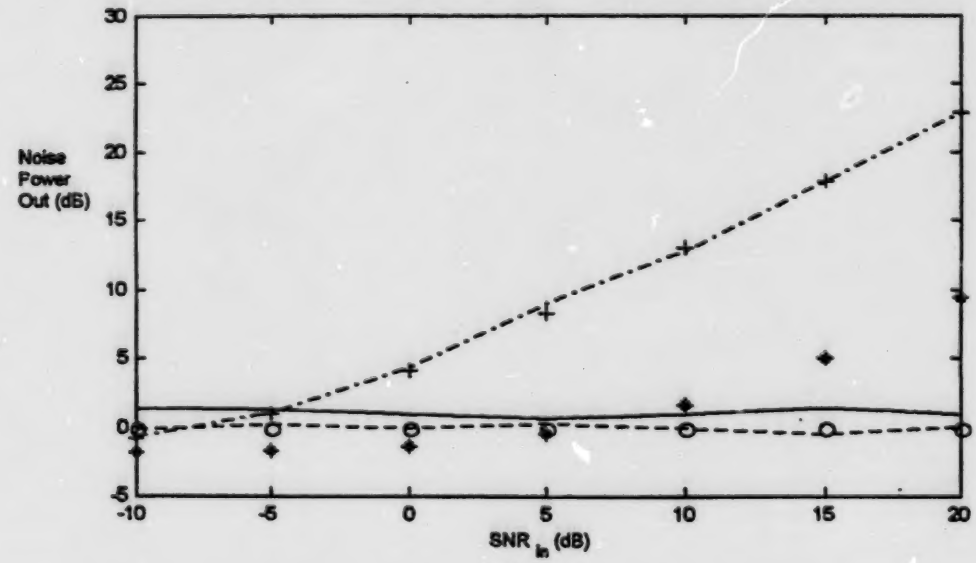

Fig 3.8 Output power at noise-only frequency for SA1-QC beamformer
(- - and o) = Hamming CB, (__ and *) = SA1-QC, (-.-. and +) = NBMV.

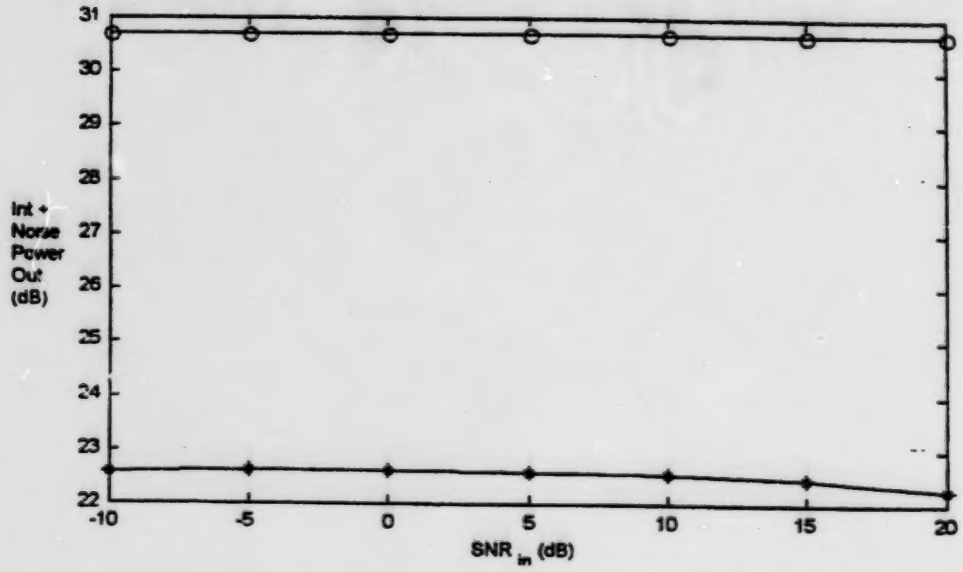

Fig. 3.9 Output power at the interference plus noise frequency for SA1-QC beamformer ooo = Hamming-CB, *** = SA1-QC beamformer. (Note vertical scale).

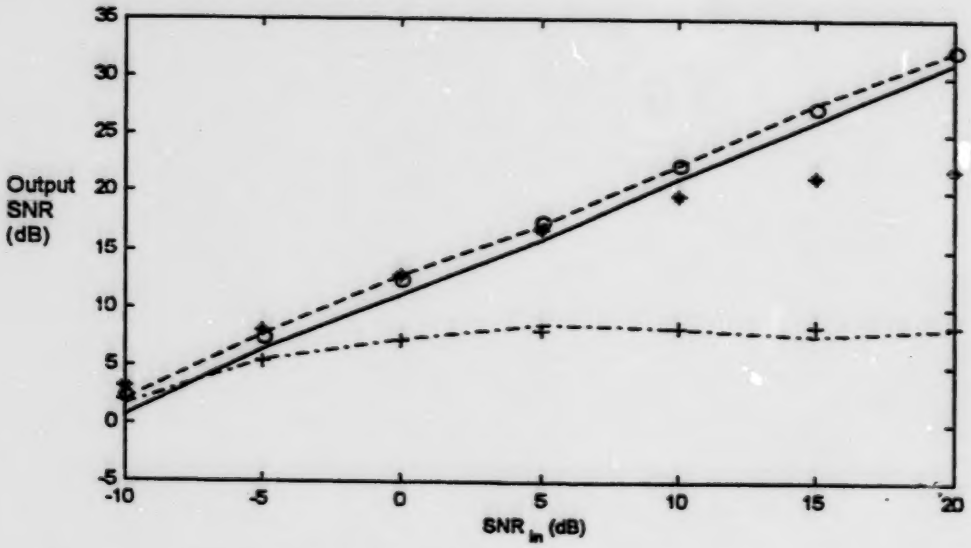

Fig 3.10 Output SNR from SA2M-QC beamformer
(- - and o) = Hamming CB, (__ and *) = SA2M-QC, (-.-. and +) = NBMV.

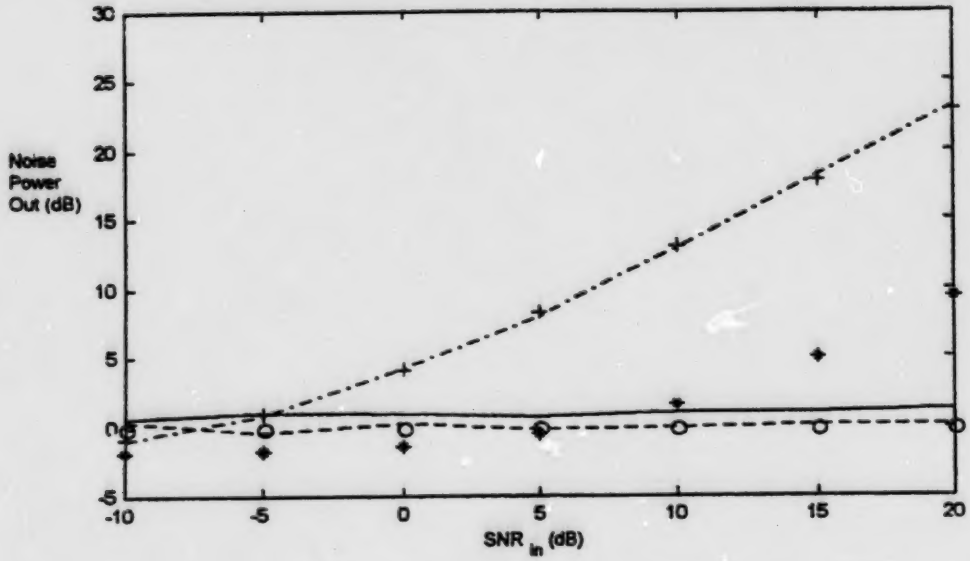

Fig 3.11 Output power at noise-only frequency for SA2M-QC beamformer
(- - and o) = Hamming CB, (__ and *) = SA2M-QC, (-.-. and +) = NBMV.

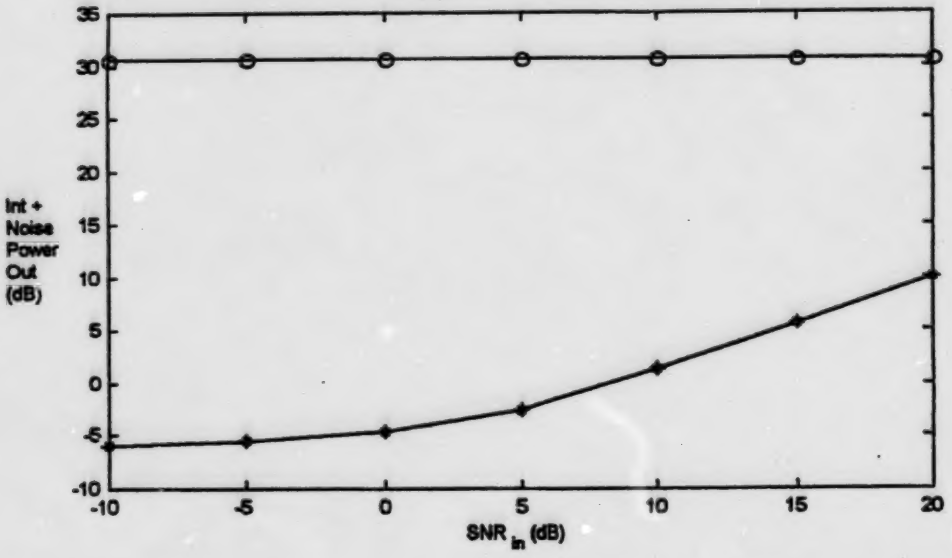

Fig 3.12 Output power at interference plus noise frequency for SA2M-QC beamformer.
ooo = Hamming-CB, *** = SA2M-QC beamformer.

4. Detection Index Experiments

4.1 Introduction

The detection index (DI) is a simple measure for evaluating the detection performance of a beamformer. The DI attempts to quantify detection performance by calculating the difference in the output power levels measured (a) in the presence of noise alone and (b) with both signal and noise present. This difference is then divided by the standard deviation of the noise-only background. If the ratio is large then there is little probability that the mean signal plus noise output level will be exceeded, by chance, by a random sample from the noise-only background and hence, in this situation, the presence of the signal is unlikely to be confused with the normal fluctuations in background measurements. In the experiments that follow we shall examine the impact of the finite-time misadjustment effect on the detection of a signal of varying strength in the presence of another signal at the same bearing (but at a different temporal frequency) and in the presence of an interferer at yet a third frequency and at a different bearing.

4.2 Detection Index Experiments

(A) Two signals with same bearing but different frequencies

We will take an approach to calculating the DI which explicitly recognises that the SA beamformer is inherently a wideband (WB) system and hence it is possible for it to be confronted by two NB "signals" in the pre-steered direction at different temporal frequencies and with different strengths. This is of concern as we know that the finite-time misadjustment effect is strongly dependent on signal strength. Hence, for instance, we should examine the detection performance for a weak signal in the presence of a strong one at the same bearing.

As previously, the simulation is constructed for an N =24 sensor array with M =24 FFT bins (i.e. 24 temporal frequencies , or 24 Fourier vectors). We have "signal" at two of these frequencies with input SNR's measured "in the bin" at the sensor level of SNR1 and SNR2. The background noise is spatially and temporally uncorrelated.

The detection index is calculated in dB for signal #2 as

$$DI = 10\log\left(\frac{E(P_{s+n}) - E(P_n)}{std(P_n)}\right)$$

where P_{s+n} is the estimate of the signal plus noise power output "in the bin" for signal #2 calculated from a single realisation of the 24 by 24 data matrix, and P_n is the corresponding estimate of the noise-only power in the same bin. For the latter calculation, the strength of signal #2 is deliberately set to zero. The statistics $E(P_n)$, $E(P_{s+n})$, and $std(P_n)$ are each estimated from 800 realisations of each scenario.

In Fig. 4.1 we compare the DI values for the SA1 (solid curves) and SA2M (dashed curves) ABF's. The figure is complicated as we not only have two beamformers but for each of these we have four values of SNR2, and for each of these we have four values of adaptive degrees of freedom (DOF)[1]. The horizontal axis is SNR1, the SNR of the "other" signal co-located in bearing. Because of its complexity, Fig. 4.1 will be discussed in some detail, as follows.

For a given value of SNR1, we actually use five values of SNR2 = {-∞, -10, -5, 0, +5}dB. The first relates to zero signal strength for signal #2 and is used to establish the value of $E(P_n)$ and $std(P_n)$. The other four give rise to the four major families of curves

[1] Recall that DOF = N_s - 1 where N_s is the number of subarrays.

that are most easily discerned by looking at the left hand side of the figure. The uppermost family is grouped about DI=18dB and relates to SNR2 = 5dB. The other three families are observed to lie at multiples of about 5dB below this set and correspond to the three lower values of SNR2. Within each family we have four values of DOF ={0, 1, 3, 6}. A DOF of zero implies a non-adaptive, unshaded CB and is included as a baseline measurement. For each value of DOF the DI statistics were computed separately.

Let us concentrate initially on the uppermost family, SNR2 = 5dB. As a starting point we observe that each solid line (SA1) is fairly well paired with a dashed line (SA2M) indicating that under similar conditions both beamformers offer very similar performance. As we move towards the right of the figure (increasing SNR1 and hence increasing misadjustment effects related to SNR1) the curve family splits into 4 distinct SA1/SA2M pairs. The uppermost pair continues more or less horizontally across the graph; these are the results for DOF =0, or the CB. Obviously we do not expect these to be subject to misadjustment effects. In passing we might note that for an unshaded CB, DI = 10log(N)+ SNR2= 18.9dB, (assuming SNR2 is in decibels) which agrees with the level observed in Fig. 4.1. We further observe that the curves with the highest DOF are most susceptible to loss of DI due to increasing values of SNR1. At SNR1 = 20dB, the DI for SNR2 =5dB, DOF = 6, has dropped to about 4dB.

As we lower the value of SNR2, the curve family simply translates downwards by the corresponding amount.

In summary we can say that these results suggest that the SA1 and SA2M adaptive beamformers offer similar detection performances which are deleteriously affected by increasing the number of adaptive DOF and the level of the "other" signal. The SNR-related effects are dominant. These adverse effects are largely unaffected by the strength of the signal itself.

We now move on to Fig. 4.2 which is a repeat of the above experiment but with a quadratic constraint (QC) applied to both ABF's to limit the weight norm to a maximum of 2/N. Recall that the unity gain unshaded CB has a weight norm of 1/N [3-1].

The results of Fig. 4.2 again cluster into four families, but unlike those of Fig. 4.1, they suffer little deterioration as SNR1 increases. This is to be expected as the whole purpose of the QC approach is to limit the misadjustment effect. Again the impact of varying SNR2 is a simple vertical translation of the entire curve family.

(B) Two signals and a close interferer.

Adding a close NB interferer with a spatial frequency π/N (i.e. at ½ CB beamwidth from the signal(s)) and an INR of 10dB yields the results of Fig. 4.3 for the SA1 and SA2M beamformers. It has the same overall structure as Fig. 4.1 though for low values of SNR1 we note that the SA1 curves (solid lines) are a dB or so lower than the SA2M and that both are lower than on Fig. 4.1 (for DOF>0). This indicates that, while the detection performances of both ABF's are affected by the interference, the SA1 BF is the more affected. This remains true as SNR1 increases. Indeed we see that for DOF = 1 the SA2M curve remains horizontal while the SA1 curve drops noticeably for higher SNR1.

Running the QC versions of both beamformers results in Fig. 4.4. Again we see that there is a decrease in DI of approximately 2dB (w.r.t CB) due to the impact of the interferer, but in this case both the SA1-QC and the SA2M-QC have roughly equal performances which are little affected by changes in SNR1.

Increasing the INR of the interferer to 20dB yields the SA1 and SA2M results of Fig. 4.5. At low SNR1, where the misadjustment effect is modest, we see that the SA2M results are now about 3dB worse than the CB, while the SA1 results are about 6dB worse. In this situation, the SA2M ABF is clearly superior to the SA1 beamformer. Increasing

SNR1 has a similar impact to that observed previously. However, in this case, for DOF =1 both beamformers are little affected by changes in SNR1.

The QC versions of both beamformers have DI values plotted in Fig. 4.6. As we have seen in Figs. 4.2 and 4.4, we again have relatively flat response curves where the SA1-QC and SAM2-QC perform similarly. The level of performance is about that of SA2M on Fig. 4.5 for low SNR1.

4.3 Summary

The experiments performed here indicate that the SA1 and SA2M beamformers have detection performances which are for the most part comparable. Both suffer from misadjustment problems associated with a strong signal co-located in bearing. Where there are noticeable differences, for example with a very strong interferer, the SA2M is superior.

When the experiments are re-run with quadratically-constrained versions of the two beamformers, the performance of each improves and there are no noticeable differences in performance between the two adaptive beamformers. The misadjustment effect is largely eliminated.

Overall, it would seem that as the SA2M is superior to the SA1, and the SA1-QC and SA2M-QC are similar in performance, then if one had to specify the best overall subarray geometry, it would be that of the modified-Owsley geometry of the SA2M/SA2M-QC.

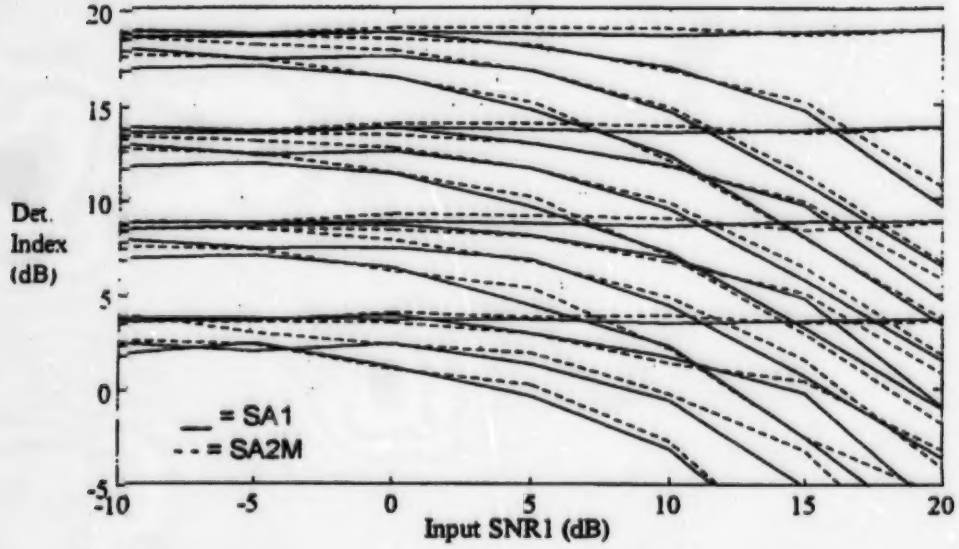

Fig. 4.1. SA1 and SA2M detection index. Little difference in performance. See text for details.

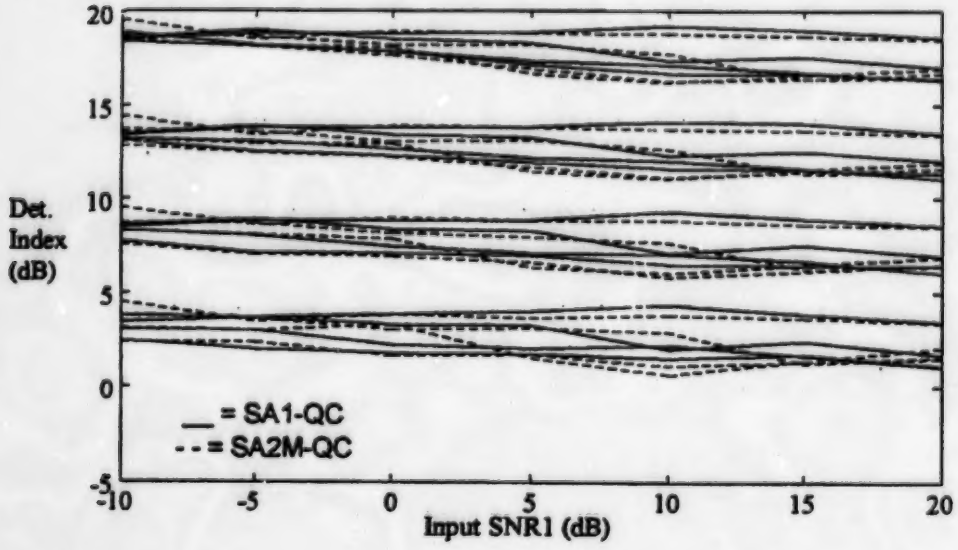

Fig. 4.2. SA-QC and SA2M-QC detection index. Note improvement over Fig. 4.1.

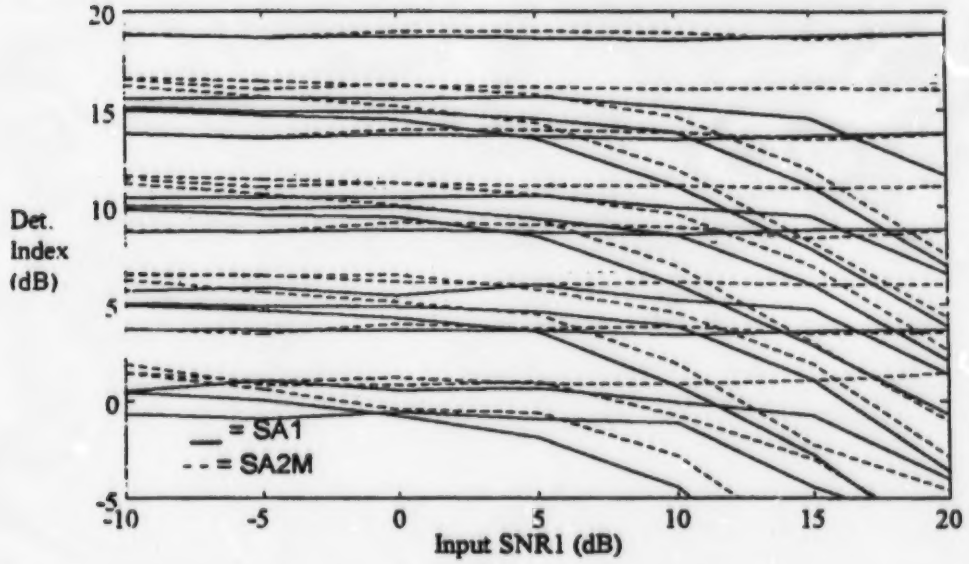

Fig. 4.3. As Fig. 4.1 but with presence of close interferer with INR = 10dB.

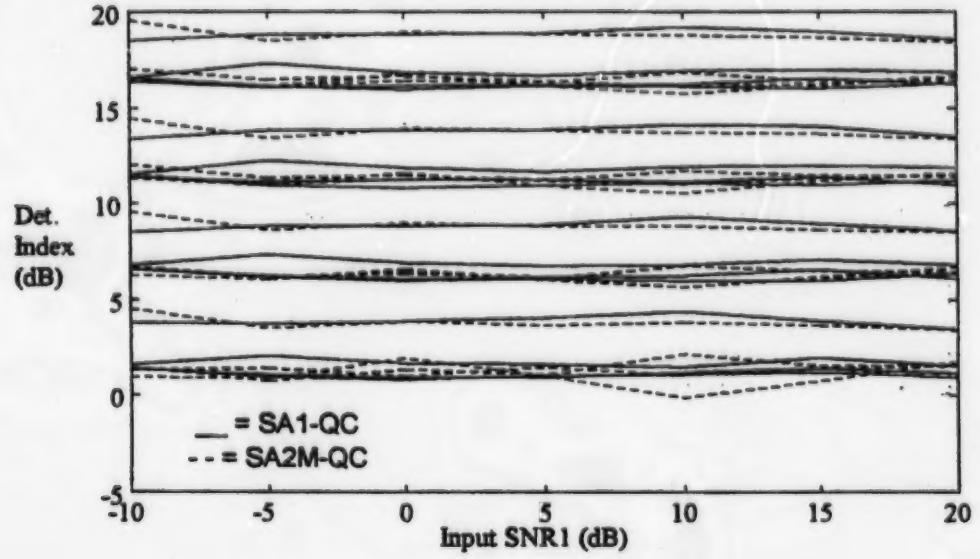

Fig 4.4. As Fig. 4.3 but with SA1-QC and SA2M-QC beamformers. Again note improvement over Fig. 4.3.

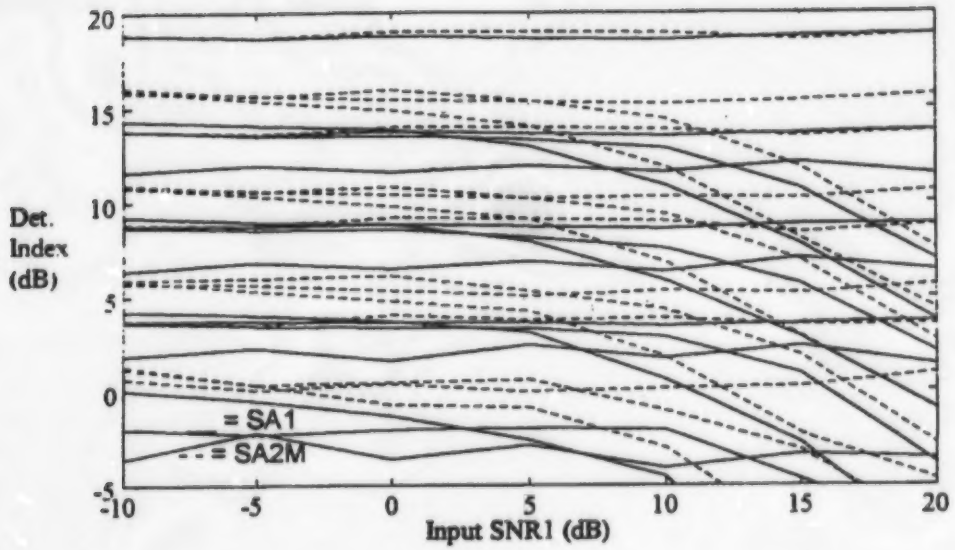

Fig. 4.5. As Fig. 4.1 but with close interferer with INR = 20dB.

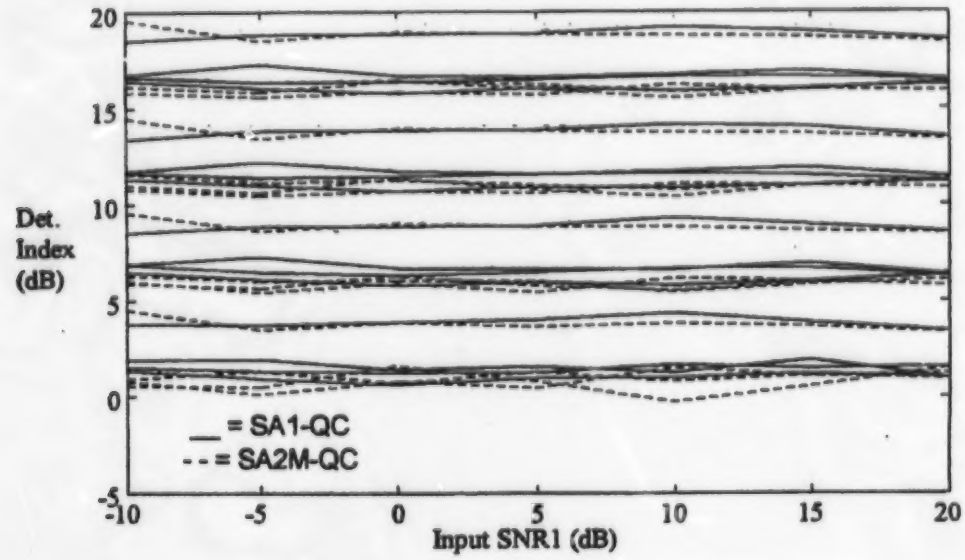

Fig .4.6. As Fig. 4.5 but with SA1-QC and SA2M-QC beamformers.

5. Conclusion

It has been demonstrated that, due to their regular geometry, the SA1 and SA2 STMV-SA beamformers are subject to grating lobe-type phenomena which degrades their performance at certain bearings. This effect is ameliorated by using beamformers with irregular geometries (SA2M, SAX) but the SAX is inferior in terms of dealing with "close" interferences.

Overall, the results suggest that, of the four SA beamformers under investigation, the SA2M beamformer seems to offer the best combination of freedom from artifacts together with the ability to deal with close interferences. However, it should be stressed that the SA beamformers, as members of the MVDR class, still suffer from the classic multipath signal-cancellation problem where two (or more) signals are received at the same frequency. On the other hand, in the absence of multipath, we have demonstrated that the MVDR-SA's output SNR in the finite-time case can be considerably better than that of the corresponding narrowband MVDR beamformer, notwithstanding the fact that the observation time is shorter for the SA beamformer.

This report has also elucidated some of the performance benefits of the quadratically-constrained versions of the SA beamformer(s).

6. References

[1-1] Swingler, D. N., "Steered adaptive subarray beamforming", DREA Contractor Report, 1997

[1-2] Dhanatawari, A. C., "Adaptive beamforming with near-instantaneous convergence in a passive and active sonar systems [sic]," DREA Contractor Report, CR96/450, June 1996.

[1-3] Owsley, N. L, "Systolic array beamforming", NUSC Report, 7891, Sept. 1987.

[3-1] Swingler, D. N., "Robust adaptive beamforming", DREA Contractor Report, CR/96/450, June 1996

DOCUMENT CONTROL DATA

(Security classification of title, body of abstract and indexing annotation must be entered when the overall document is classified)

1. ORIGINATOR (the name and address of the organization preparing the document. Organizations for whom the document was prepared, e.g. Establishment sponsoring a contractor's report, or tasking agency, are entered in section 8.)

Division of Engineering
Saint Mary's University
Halifax, NS B3H 3C3

2. SECURITY CLASSIFICATION (overall security classification of the document including special warning terms if applicable).

UNCLASSIFIED

3. TITLE (the complete document title as indicated on the title page. Its classification should be indicated by the appropriate abbreviation (S,C,R or U) in parentheses after the title).

Detection Performance of the Steered, Adaptive, Subarray Beamformer

4. AUTHORS (Last name, first name, middle initial. If military, show rank, e.g. Doe, Maj. John E.)

Swingler, David N.

5. DATE OF PUBLICATION (month and year of publication of document)

January 1999

6a. NO. OF PAGES (total containing information Include Annexes, Appendices, etc).

34

6b. NO. OF REFS (total cited in document)

4

7. DESCRIPTIVE NOTES (the category of the document, e.g. technical report, technical note or memorandum. If appropriate, enter the type of report, e.g. interim, progress, summary, annual or final. Give the inclusive dates when a specific reporting period is covered).

Contractor Report

8. SPONSORING ACTIVITY (the name of the department project office or laboratory sponsoring the research and development. Include address).

Defence Research Establishment Atlantic, P.O. Box 1012, Dartmouth, NS B2Y 3Z7

9a. PROJECT OR GRANT NO. (if appropriate, the applicable research and development project or grant number under which the document was written. Please specify whether project or grant).

Project 1cc11

9b. CONTRACT NO. (if appropriate, the applicable number under which the document was written).

W7707-7-5425

10a ORIGINATOR'S DOCUMENT NUMBER (the official document number by which the document is identified by the originating activity. This number must be unique to this document.)

10b OTHER DOCUMENT NOs. (Any other numbers which may be assigned this document either by the originator or by the sponsor.)

DREA CR 1999-004

11. DOCUMENT AVAILABILITY (any limitations on further dissemination of the document, other than those imposed by security classification)

(x) Unlimited distribution
( ) Defence departments and defence contractors; further distribution only as approved
( ) Defence departments and Canadian defence contractors; further distribution only as approved
( ) Government departments and agencies; further distribution only as approved
( ) Defence departments; further distribution only as approved
( ) Other (please specify):

12. DOCUMENT ANNOUNCEMENT (any limitation to the bibliographic announcement of this document. This will normally correspond to the Document Availability (11). However, where further distribution (beyond the audience specified in (11) is possible, a wider announcement audience may be selected).

Unlimited

13. ABSTRACT (a brief and factual summary of the document. It may also appear elsewhere in the body of the document itself. It is highly desirable that the abstract of classified documents be unclassified. Each paragraph of the abstract shall begin with an indication of the security classification of the information in the paragraph (unless the document itself is unclassified) represented as (S), (C), (R), or (U). It is not necessary to include here abstracts in both official languages unless the text is bilingual).

The detection performance of the steered, minimum variance, subarray beamformer is examined via numerical simulations, with specific reference to the impact of four different subarray geometries. Additionally the advantages of employing a quadratic constraint are examined. The measures used to elucidate performance include output SNR, array gain, and the detection index. The most salient result is that the beamformer with contiguous subarrays of differing lengths (referred to herein as SA2M), and its quadratically-constrained counterpart, appear to offer the best overall performance in terms of their ability to null close interferers while offering freedom from the type of artifacts that potentially bedevil the other subarray beamformers under test.

14. KEYWORDS, DESCRIPTORS or IDENTIFIERS (technically meaningful terms or short phrases that characterize a document and could be helpful in cataloguing the document. They should be selected so that no security classification is required. Identifiers, such as equipment model designation, trade name, military project code name, geographic location may also be included. If possible keywords should be selected from a published thesaurus. e.g. Thesaurus of Engineering and Scientific Terms (TEST) and that thesaurus-identified. If it not possible to select indexing terms which are Unclassified, the classification of each should be indicated as with the title).

signal processing
sonar
beamforming
adaptive systems
detection